Spectrochimica Acta Part A: Molecular and Biomolecular Spectroscopy 121 (2014) 306–312

Contents lists available at ScienceDirect

Spectrochimica Acta Part A: Molecular and Biomolecular Spectroscopy

journal homepage: www.elsevier.com/locate/saa

Synthesis and evaluation of simple naked-eye colorimetric chemosensors for anions based on azo dye-thiosemicarbazones

Widchaya Radchatawedchakoon, Withsakorn Sangsuwan, Senee Kruanetr, Uthai Sakee *

Center of Excellence for Innovation in Chemistry (PERCH-CIC), Department of Chemistry, Faculty of Science, Mahasarakham University, Mahasarakham 44150, Thailand

HIGHLIGHTS

- New azo dye-thiosemicarbazone derivatives were synthesized for anion sensor evaluation.
- It is a very good naked eye detection sensor.
- The sensor has detection limit of 0.71 μM for acetate.

GRAPHICAL ABSTRACT

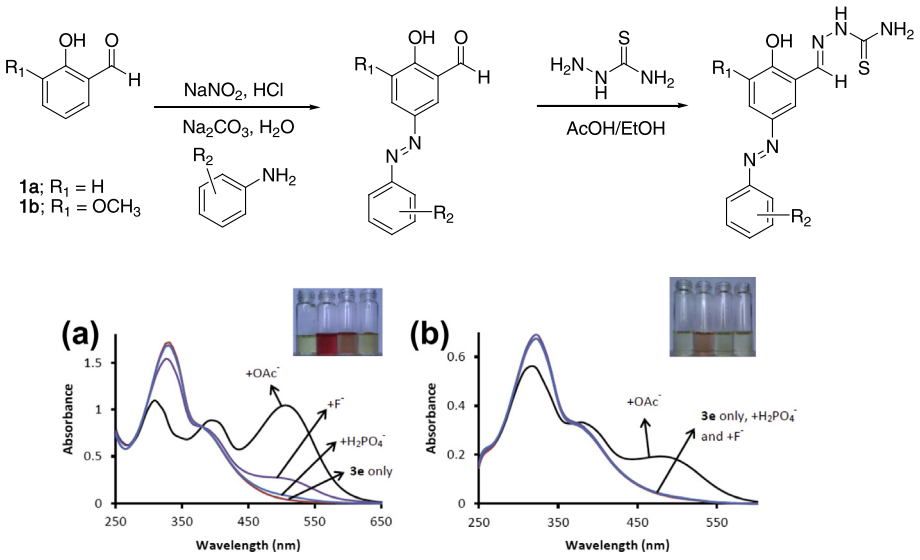

ARTICLE INFO

Article history:
Received 25 July 2013
Received in revised form 7 October 2013
Accepted 15 October 2013
Available online 4 November 2013

Keywords:
Azo
Thiosemicarbazone
Anion
Sensor

ABSTRACT

A series of novel, highly selective azo dye-thiosemicarbazones based anion sensors (**3e**–**f**) have been synthesized from the condensation reaction between thiosemicarbazide and six different azo salicylaldehydes. The structure of the sensors was confirmed by spectroscopic methods. The selectivity and sensitivity in the recognition for acetate anion over other anions such as fluoride, chloride, iodide and dihydrogenphosphate anions were determined by naked-eyes and UV–vis spectra. The color of the solution containing sensor had an obvious change from light yellow to orange only after the addition of acetate anion in aqueous solution (water/dimethylsulfoxide, 7:3, v/v) while other anions did not cause obvious color change. The anion recognition property of the receptor via proton-transfer is monitored by UV–vis titration and ^{1}H NMR spectroscopy. Under condition in aqueous solution of sensor **3e** (water/dimethylsulfoxide, 7:3, v/v), linearity range for the quantification of acetate anion was 1–22 μM and limit of detection (LOD) of acetate anion was 0.71 μM.

* Corresponding author. Address: Department of Chemistry, Faculty of Science, Mahasarakham University, T. Khamrieng, A. Kantarawichai, Mahasarakham 44150, Thailand. Tel./fax: +66 43 754246.
E-mail address: uthai.s@msu.ac.th (U. Sakee).

1386-1425/$ - see front matter © 2013 Elsevier B.V. All rights reserved.
http://dx.doi.org/10.1016/j.saa.2013.10.086

Introduction

It is well known that azo colorants are the most versatile class of dyes [1]. While compounds with a thiosemicarbazone structure and their transition metal complexes have a wide range of biological activities, some of them are antiviral [2], antifungal [3], antibacterial [4], antitumor [5], antioxidant [6], analgesic and anti-inflammatory properties [7]. Such thiosemicarbazones have been reported to be useful as chemosensors [8]. The design of host molecules that can recognize and sense anions selectively through visible has received considerable interest in recent years because of the important roles played by the anions in biological, industrial, and environmental processes [9]. In biological and environmental systems, anion–sensor interactions commonly occur in aqueous solution, therefore, much attention has been paid to developing anion sensors that work in the aqueous phase [10]. It is still a challenge to design the anion sensors with high selectivity and sensitivity in a competitive media. As a subset of the anion receptor, the chromogenic anion sensors have shown unique merit, because they can reveal the host-anion binding information through a change of color [11]. Generally colorimetric chemosensor is made up of two main fragments, which involve the binding sites that interact with anions either electrostatically or through hydrogen bonding and the signal parts that connect to the binding sites either directly or intramolecularly linked which show the color changes in the anion recognition procession [12].

The sensors based on colorimetric determination of anions are still challenges for investigators and they attract much interest. In particular, to develop the naked-eye detection technique for the analytes without using any expensive equipment is of great interest in recent years.

In this paper, we designed and synthesized new and simple anion receptors **3a**–**f** containing both azo dye and thiosemicarbazone unit and studied their anion recognition behaviors. In addition, the sensing processes can be realized by the 'naked-eye' determination as it has a remarkable color response.

Experiment

General

All solvents and reagents were purchased from commercial sources and used as received. IR spectra were recorded on Perkin Elmer SPECTRUM GX, FT-IR spectrophotometer. Spectra were recorded as pressed KBr disc. The ^{1}H and ^{13}C NMR spectra were measured with a Bruker AVANCE 400 spectrometer operating at 400 and 100 MHz, respectively. The chemical shifts (δ) are reported in ppm, and coupling constants (J) are given in Hz. The spectra were taken in CD_3SOCD_3 and the residual solvent signal of CH_3SOCH_3 at δ 2.50 and 39.5 was used as reference for ^{1}H and ^{13}C NMR spectra. The HRMS mass spectra were recorded on micrOTOF spectrometer.

Synthesis

*General procedure for sensors **3a–f** synthesis*

*Synthesis derivatives of azo aromatic aldehyde **2a–f**.* The structures of synthesized azo aromatic aldehyde are shown in Scheme 1. A 0 °C solution I of aniline derivatives (10 mmol) in deionized (DI) water (10 mL) and HCl (2 mL) was prepared. A 0 °C solution II of $NaNO_2$ (15 mmol) in DI water (5 mL) was dropwised into the solution I. The mixture was stirred for 10 min. A solution of Na_2CO_3 (30 mmol) in DI water (30 mL) at 0 °C was added aldehyde derivatives **1a** or **1b** (10 mmol). The solution of aldehyde derivatives and Na_2CO_3 was dropwised into the mixture solution of I and II and then the solution was stirred 2 h in cool bath. The reaction was adjusted the pH to 7 by adding the solution of HCl. The precipitated products **2a**–**f** were filtered and heated in the oven.

*Synthesis derivatives of thiosemicarbazone **3a–f**.* Thiosemicarbazone (1 mmol) was added into the solution of azo aromatic aldehydes **2a**–**f** (1 mmol) in ethanol (10 mL) and acetic acid (10 drops). The reaction was stirred and refluxed for 6–7 h. After heating, the precipitated products **3a**–**f** were filtered and heated in the oven.

*Sensor **3a***

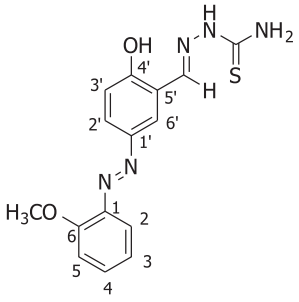

Yield: 99.91%, m.p. = 197–210 °C. IR (KBr, cm^{-1}); 3432, 3256, 3162, 1602, 1514, 1559, 1107, 762. ^{1}H NMR (d_6-DMSO,

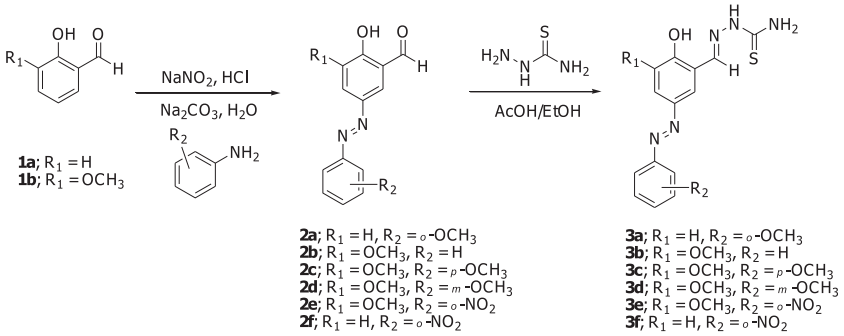

Scheme 1. Synthetic procedures for sensors **3a**–**3f**.

400 MHz): δ 3.93 (s, 3H), 7.02 (m, 2H, H-2 and H-5), 7.24 (m, 1H, H-2′), 7.47 (m, 2H, H-3 and H-4), 7.71 (d, J = 8.7 Hz, 1H, H-3′), 8.08 and 8.15 (br s, 2H, NH_2), 8.45 (s, 1H, Ar—CH=N—), 8.52 (s, 1H, H-6′), 11.48 (s, 1H, OH). ^{13}C NMR (d_6-DMSO, 100 MHz): δ 55.9 (OCH_3), 113.3, 116.3, 116.8, 120.4, 120.9, 122.3, 124.8, 132.1, 138.7, 141.6, 145.9, 156.2 (aromatic carbons), 159.0 (C=N), 177.8 (C=S). HRMS (+eV): m/z (% rel. intensity): 330.1005 $[M + H]^+$ (100).

Sensor ***3b***

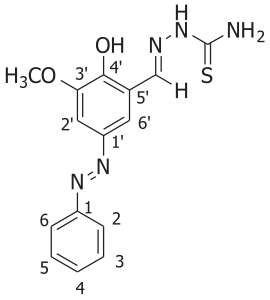

Yield: 58.92%, m.p. = 223 °C. IR (KBr, cm^{-1}); 3306, 1601, 1531, 1559, 1111, 766, 686. ^{1}H NMR (d_6-DMSO, 400 MHz): δ 3.91 (s, 3H, OCH_3), 7.42 (s, 1H, H-2′), 7.51 (m, 3H, H-3,4,5), 7.84 (d, J = 7.5 Hz, H-2 and H-6), 8.10 and 8.16 (br s, 2H, NH_2), 8.30 (br s, 1H, Ar—CH=N), 8.48 (br d, J = 2.2 Hz, 1H, H-6′), 11.49 (br s, 1H, OH). ^{13}C NMR (d_6-DMSO, 100 MHz): δ 56.0 (OCH_3), 101.3, 119.1, 120.8, 122.1, 129.3, 130.6, 138.4, 144.9, 148.7, and 149.4 (aromatic carbons), 152.0 (Ar—C=NH–), 177.9 (C=S). HRMS (+eV): m/z (% rel. intensity): 352.0831 $[M + Na]^+$ (100).

Sensor ***3c***

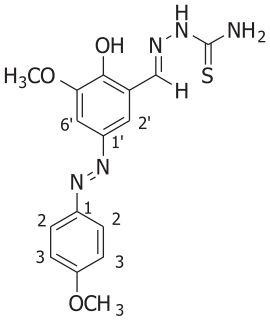

Yield: 45.63%, m.p. = 235–236 °C. IR (KBr, cm^{-1}); 3356, 1596, 1503, 1539, 1123, 834. ^{1}H NMR (d_6-DMSO, 400 MHz): δ 3.87 and 3.92 (s, 6H, 2 × OCH_3), 7.07 (d, J = 7.9 Hz, 2H, H-3), 7.37 (s, 1H, H-6′), 7.81 (d, J = 8.4 Hz, 2H, H-2), 8.05 and 8.13 (br s, 2H, NH_2), 8.19 (s, 1H, Ar—CH=N—), 8.45 (s, 1H, H-2′), 11.46 (s, 1H, OH). ^{13}C NMR (d_6-DMSO, 100 MHz): δ 55.5 and 55.9 (2 × OCH_3), 101.4, 114.5, 118.2, 120.7, 124.0, 138.5, 144.9, 146.1, 148.6 and 148.8 (aromatic carbons), 161.3 (Ar—CH=N—), 177.8 (C=S). HRMS (+eV): m/z (% rel. intensity): 360.1104 $[M + Na]^+$ (100).

Sensor ***3d***

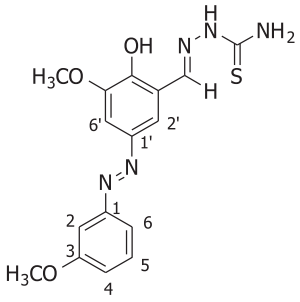

Yield: 75.95%, m.p. = 215 °C. IR (KBr, cm^{-1}); 3451, 3366, 3325, 1601, 1469, 1532, 1129, 864, 827, 787. ^{1}H NMR (d_6-DMSO, 400 MHz): δ 3.82 and 3.90 (s, 6H, 2 × OCH_3), 7.06 (br s, 1H, H-4), 7.42 (br m, 4H, H-2,5,6 and 6′), 8.11 and 8.17 (br s, 2H, NH_2), 8.31 (s, 1H, Ar—CH=N—), 8.48 (s, 1H, H-2′), 11.50 (s, 1H, OH). ^{13}C NMR (d_6-DMSO, 100 MHz): δ 55.3 and 55.9 (2 × OCH_3), 101.2, 105.7, 115.8, 116.9, 119.4, 120.7, 130.1, 138.4, 144.6, 148.8, 149.9 and 153.3 (aromatic carbons), 160.0 (Ar—CH=N—), 177.8 (C=S). HRMS (+eV): m/z (% rel. intensity): 382.0938 $[M + Na]^+$ (100).

Sensor ***3e***

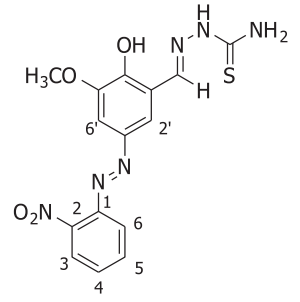

Yield: 55.09%, m.p. = 213 °C. IR (KBr, cm^{-1}); 3338, 1605, 1474, 1529, 1128, 753. ^{1}H NMR (d_6-DMSO, 400 MHz): δ 3.89 (s, 3H, OCH_3), 7.28 (s, 1H, H-6′), 7.69 (d, 1H, J = 7.6 Hz, H-6), 7.69 (t, 1H, J = 7.6 Hz, H-4), 7.82 (t, 1H, J = 7.6 Hz, H-5), 8.07 (d, 1H, J = 7.6 Hz, H-3), 8.10 (s, 1H, H-2′), 8.17 and 8.38 (s, 2H, —NH_2), 8.45 (s, 1H, Ar—CH=N—), 11.51 (s, 1H, OH). ^{13}C NMR (d_6-DMSO, 100 MHz): δ 55.9 (OCH_3), 100.7, 118.7, 120.9, 121.1, 124.2, 130.6, 133.6, 138.0, 144.6, 144.9, 146.4 and 148.9 (aromatic carbons), 150.9 (C=N), 177.9 (C=S). HRMS (+eV): m/z (% rel. intensity): 397.0670 $[M + Na]^+$ (100).

*Sensor **3f***

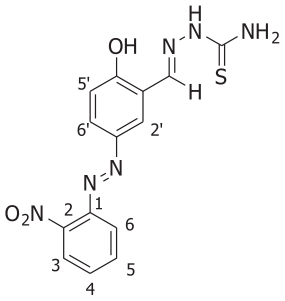

Yield: 95.57%, m.p. = 194–197 °C. IR (KBr, cm^{-1}); 3508, 3160, 2981, 2367, 1595, 1559, 1534, 1488, 1353, 1280, 1160, 1112. ^{1}H NMR (d_6-DMSO, 400 MHz): δ 7.07 (d, J = 8.6 Hz, 1H, H-5′), 7.67 (m, 3H, H-6′, 4 and 5), 7.83 (m, 1H, H-6), 8.08 (br d, J = 6.0 Hz, 2H, NH_2), 8.19 (s, 1H, Ar—CH═N—), 8.44 (s, 1H, H-2′), 8.63 (s, 1H, H-3), 11.51 (s, 1H, OH). ^{13}C NMR (d_6-DMSO, 100 MHz): δ 117.6, 119.0, 121.7, 122.8, 124.5, 126.5, 131.2, 133.9, 138.5, 144.9, 145.9 and 147.1 (aromatic carbons), 160.8 (C═N), 178.3 (C═S).

General procedure for UV–vis experiments

Deionized water was used throughout all experiments. All UV–vis spectroscopy was carried out just after the addition of anions in DMSO or a DMSO/H_2O binary solution, while keeping the sensor concentration constant (2.0×10^{-5} M) on a Perkin Elmer Lambda25 UV–vis spectrometer. All anions (AcO^-, F^-, Cl^-, Br^-, I^- and $H_2PO_4^-$) were used as tetra-*n*-butylammonium salts.

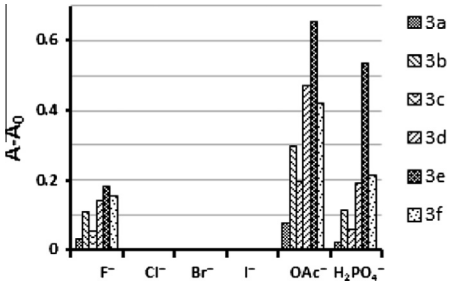

Fig. 2. Comparison of relative absorbance at 510 nm of sensor **3a–f** to various anions.

Results and discussion

The synthesis of **3a–f** were obtained in good yields by simple condensation reactions between aldehyde and amine, followed by coupling with thiosemicarbazide. The chemical structures of the newly prepared compounds were confirmed by ^{1}H NMR, ^{13}C NMR and HRMS spectra data (Scheme 1).

The colorimetric sensing abilities were primary investigated by adding various anions such as F^-, Cl^-, Br^-, I^-, AcO^- and $H_2PO_4^-$ (tetrabutyl ammonium was used as a countercation) to DMSO solutions of sensors **3a–f** (2×10^{-5} M). The addition of 5 equiv. of Cl^-, $Br^-$and I^- anions did not result in any color or spectrum

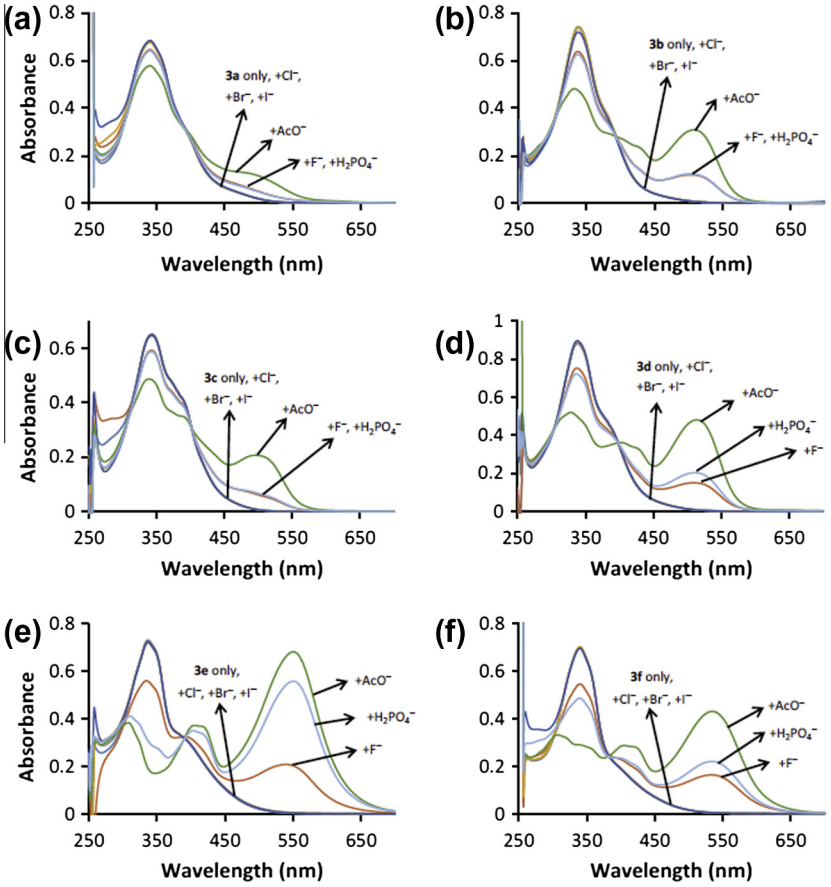

Fig. 1. UV–vis absorption spectra of **3a–e** (2.0×10^{-5} M) in the presence of 10 equiv of various anions in DMSO; (a) **3a**, (b) **3b**, (c) **3c**, (d) **3d**, (e) **3e** and (f) **3f**.

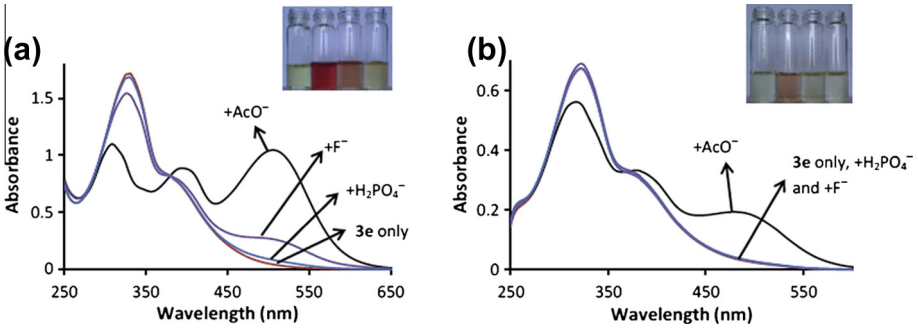

Fig. 3. UV–vis absorption changes of **3e** with various anions (10 equiv); (a) **3e** = 5×10^{-5} M in 2:3 H_2O/DMSO and (b) **3e** = 2×10^{-5} M in 7:3 H_2O/DMSO.

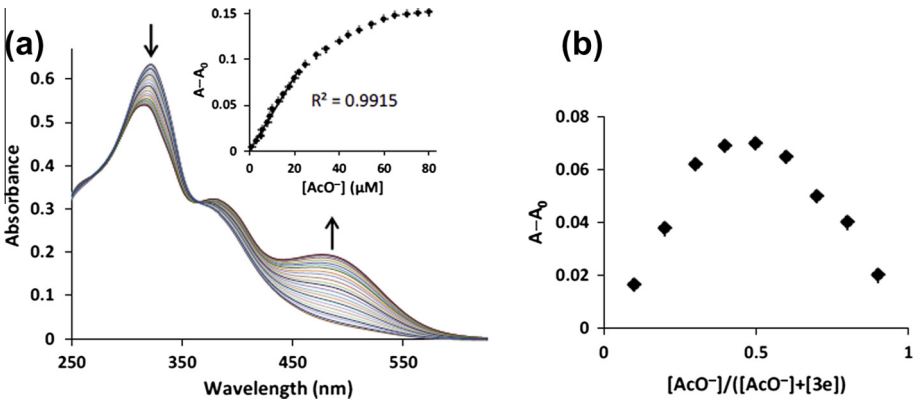

Fig. 4. (a) UV–vis spectrum changes of **3e** (2×10^{-5} M) upon addition of acetate anion (0–4 equiv.) in 7:3 H_2O/DMSO (v/v). (b) Job's plot analysis of **3e**-AcO^- complex in 7:3 H_2O/DMSO (v/v) indicates a 1:1 stoichiometry.

changes. However, it was observed that the addition of AcO^-, $H_2PO_4^-$ and F^- anions, all sensors responded with dramatic color changes from yellow to purple. In the corresponding UV–vis spectrum, a new and strong absorption peak appeared at 500–550 nm (Fig. 1). Fig. 2 shows the comparison of relative absorbance at 510 nm of sensors **3a–f** to various anions. Evidently, the changes in the absorption spectral profile of **3e** is better than other. The most remarkable color based changes were observed with azo-sensor, **3e** appended with nitrophenyl substituent. The results indicated the nitro group on the azobenzene unit could improve not only anion binding ability of **3e** but also their visible sensing ability.

In H_2O/DMSO binary solutions, as it can be anticipated, the anion sense abilities of the sensor vary with the volume ratio of water. As shown in Fig. 3a and b in H_2O/DMSO (2: 3, 7:3, v/v, respectively) solution, **3e** showed an obvious color change upon addition of AcO^-, $H_2PO_4^-$ and F^-. For AcO^-, sensor **3e** showed the color change from purple to orange in H_2O/DMSO (2: 3, 7:3, v/v) solution. Therefore, in H_2O/DMSO (7:3, v/v)) solution, sensor **3e** has the single colorimetric selectivity to AcO^-.

UV–vis titrations of **3e** were carried out in H_2O/DMSO (7:3, v/v) solution at a concentration level of 5.0×10^{-5} M upon incremental addition of tetrabutylammonium acetate up to 5 equivalents and the resulting spectra are shown in Fig. 4a. The first band in the wavelength 332 nm was assigned to the transition between the π-orbital localized on the central band of azomethine group (CH═N—). The second band located in the wavelength of 400 nm is due to an intramolecular charge transfer (CT) transition within the whole molecule [13]. This band is more important in salicylaldimine compounds which indicate the presence of strong intramolecular hydrogen bond between the hydroxyl group and the

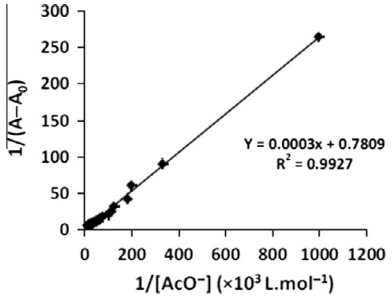

Fig. 5. Benesi–Hildebrand plot (495 nm) using Eq. (1), assuming 1:1 stoichiometry for association between **3e** and AcO^- anion.

azomethine nitrogen that causes planarity of the molecules and facilitates the charge transfer bands which are more sensitive to solvent changes than bands resulting from local transition [13]. Upon addition of AcO^-, the presence of AcO^- resulted in the intensity of the absorbance band at 332 nm decreasing gradually and the absorbance band at 400 and 495 nm increasing gradually, simultaneously accompanied with significant color changes from light yellow to orange with an isobestic point at 383 nm (Fig. 4a) indicating the sensor **3e** reacted with AcO^- and formed stable complex.

The stoichiometry between the sensor **3e** and acetate was determined by Job's plot with a total concentration of 20 μM, which showed evident 1:1 stoichiometry for small quantities of acetate in aqueous solutions (H_2O/DMSO, 7:3, v/v) (Fig. 4b).

The association constant of **3e** with AcO^- was calculated based on the UV–vis titration through the Benesi–Hildebrand equation [14], which was given as follows:

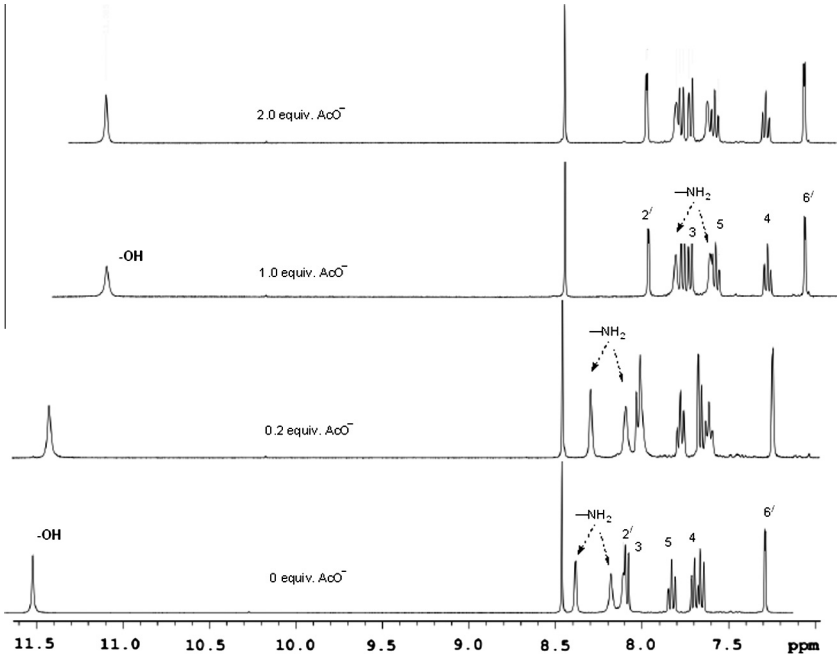

Fig. 6. Partial ^{1}H NMR titration of **3e** (0.05 M) in DMSO-d_6 with [BuN_4]OAc.

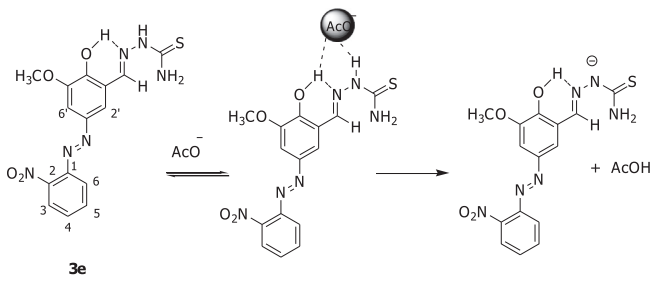

Scheme 2. Proposed host–guest binding mode of **3e** and AcO^-.

$$\frac{1}{A - A_0} = \frac{1}{A_\infty - A_0}\left[\frac{1}{K[AcO^-]_0} + 1\right] \quad (1)$$

A_0, A, and A_∞ is the absorbance of free **3e**, measured with AcO^- and measured with excess amount of AcO^- at 510 nm, respectively and K is the association constant and $[AcO^-]_0$ is the concentration of AcO^- anion added. Plotting of $1/(A–A_0)$ versus $1/[AcO^-]$ showed a linear relationship (Fig. 5), which indicates that **3e** associates with OAc^- in a 1:1 stoichiometry. The association constant (K) between **3e** and AcO^- is determined from the ratio of intercept/slope to be $2.7 \times 10^3\ M^{-1}$. The limit of detection of sensor **3e** toward AcO^- was obtained according to UV–vis titration and was at least down to 0.71 μM in aqueous solution (H_2O/DMSO, 7:3, v/v). The linearity range for the quantification of acetate anion was 1–22 μM [15].

In order to investigate the biding sites of sensor **3e** for AcO^-, ^{1}H NMR spectral changes upon the addition of AcO^- as their tetrabutyl ammonium salts to the DMSO-d_6 solution of **3e** (0.05 M) were investigated with increasing amounts of AcO^- as shown in Fig. 6. The chemical shifts of the N—H proton of the amide groups, which are associated with the binding process, did not appear in the proton NMR spectrum, even before anion was added, probably due to chemical exchange with the solvent. Upon addition of 1.0 equiv of acetate, the signals of phenol —OH and —NH_2 shifted upfield from 11.51 ppm, 8.38 ppm and 8.17 ppm to 11.09 ppm, 7.79 ppm and 7.61 ppm, respectively. The signals of H_2', H_3, H_5, H_4 and H_6' shifted upfield from 8.10 ppm, 8.07 ppm, 7.82 ppm, 7.69 ppm and 7.28 ppm to 7.95 ppm, 7.76 ppm, 7.56 ppm, 7.27 ppm and 7.05 ppm, respectively. This was attributed to the increase of the electronic density of the aromatic system and caused a shielding effect, leading to progressive upfield shift of the signals [16]. In addition, owing to the through-bond effects, the signal of —OH and —NH_2 shifted upfield and stopped after adding of 1 equiv. of AcO^-, indicating that —OH and —NH_2 did not act as a biding site. These results further support our interpretation that the interaction of the anions with the sensor is mainly due to proton-transfer to the anions rather than hydrogen-bonding. It seemed that the selectivity of **3e** for AcO^- could be ascribed to the basicity of the anions in aqueous solution. Consequently, according to the results of ^{1}H NMR titration, the proposed binding mode of **3e** and AcO^- was given below in Scheme 2.

Conclusions

In summary, we have designed and synthesized sensors **3a–f** based on azo dye-thiosemicarbazones. UV–vis spectra showed that **3e** is a good sensor in selective colorimetric recognition for acetate over other anions such as F^-, Cl^-, Br^-, I^-, $H_2PO_4^-$ in aqueous solutions (H_2O/DMSO, 2:3, v/v). Naked-eyes detectable color changes and single colorimetric recognition for AcO^- were realized successfully in aqueous solution, which made it possible to detect AcO^- for practical analysis and application.

Acknowledgements

This work was financially supported by PERCH-CIC and Mahasarakham University.

References

[1] (a) M.A. Satam, R.K. Raut, N. Sekar, Dye Pigment 96 (2013) 92–103;
(b) S.M. Kumar, K. Dhahagani, J. Rajesh, K. Nehru, J. Annaraj, G. Chakkaravarthi, G. Rajagopal, Polyhedron 59 (2013) 58–68;
(c) H. Li, Z. Xiong, X. Dai, Q. Zeng, Dye Pigment 94 (2012) 55–59.
[2] A.J. Kesel, Eur. J. Med. Chem. 46 (2011) 1656–1664.
[3] Z. Zhong, B. Aotegen, H. Xu, S. Zhao, Int. J. Biol. Macromol. 50 (2012) 1169–1174.

[4] (a) S.A. Khan, P. Kumar, R. Joshi, P.F. Iqbal, K. Saleem, Eur. J. Med. Chem. 43 (2008) 2029–2034;
(b) S.A. Khan, M. Yusuf, Eur. J. Med. Chem. 44 (2009) 2270–2274.
[5] (a) M. Khandani, T. Sedaghat, N. Erfani, M.R. Haghshenas, H.R. Khavasi, J. Mol. Struct. 1037 (2013) 136–143;
(b) K. Hu, Z.-h. Yang, S.-S. Pan, H.-j. Xu, J. Ren, Eur. J. Med. Chem. 45 (2010) 3453–3458;
(c) R.A. Finch, M.-C. Liu, S.P. Grill, W.C. Rose, R. Loomis, K.M. Vasquez, Y.-C. Cheng, A.C. Sartorelli, Biochem. Pharmacol. 59 (2000) 983–991;
(d) J. Chen, Y.-w. Huang, G. Liu, Z. Afrasiabi, E. Sinn, S. Padhye, Y. Ma, Toxicol. Appl. Pharmacol. 197 (2004) 40–48;
(e) M.-X. Li, C.-L. Chen, C.-S. Ling, J. Zhou, B.-S. Ji, Y.-J. Wu, J.-Y. Niu, Bioorg. Med. Chem. Lett. 19 (2009) 2704–2706.
[6] (a) Z. Zhong, Z. Zhong, R. Xing, P. Li, G. Mo, Int. J. Biol. Macromol. 47 (2010) 93–97;
(b) S. Ghosh, A.K. Misra, G. Bhatia, M.M. Khan, A.K. Khanna, Bioorg. Med. Chem. Lett. 19 (2009) 386–389;
(c) Y. Li, Z.-Y. Yang, J.-C. Wu, Eur. J. Med. Chem. 45 (2010) 5692–5701.
[7] (a) M.M. Aly, Y.A. Mohamed, K.A.M. El-Bayouki, W.M. Basyouni, S.Y. Abbas, Eur. J. Med. Chem. 45 (2010) 3365–3373;
(b) A.B.A. El-Gazzar, M.M. Youssef, A.M.S. Youssef, A.A. Abu-Hashem, F.A. Badria, Eur. J. Med. Chem. 44 (2009) 609–624;
(c) S.A. Khan, M. Yusuf, Eur. J. Med. Chem. 44 (2009) 2597–2600.
[8] (a) S. Sharma, M.S. Hundal, G. Hundal, Tetrahedron Lett. 54 (2013) 2423–2427;
(b) S.L.A. Kumar, M.S. Kumar, P.B. Sreeja, A. Sreekanth, Spectrochim. Acta A 113 (2013) 123–129;
(c) L.E. Santos-Figueroa, M.E. Moragues, M.M.M. Raposo, R.M.F. Batista, R.C.M. Ferreira, S.P.G. Costa, F. Sancenon, R. Martínez-Manez, J. Soto, J.V. Ros-Lis, Tetrahedron 68 (2012) 7179–7186.
[9] (a) M. Xue, X. Wang, L. Duan, W. Gao, L. Ji, B. Tang, Biosens. Bioelectron. 36 (2012) 168–173;
(b) Y. Zheng, C. Tan, G.P.C. Drummen, Q. Wang, Spectrochim. Acta A 96 (2012) 387–394.
[10] (a) Y.-M. Zhang, Q. Lin, T.-B. Wei, D.-D. Wang, H. Yao, Y.-L. Wang, Sensor Actuat. B-Chem. 137 (2009) 447–455;
(b) A.K. Singh, V. Aggarwal, U.P. Singh, S. Mehtab, Talanta 77 (2008) 718–726;
(c) I.A. Azath, P. Suresh, K. Pitchumani, Sensor Actuat. B-Chem. 155 (2011) 909–914.
[11] (a) K. Ghosh, S. Adhikari, R. FrÖhlich, I.D. Petsalakis, J. Mol. Struct. 1004 (2011) 193–203;
(b) Y.M. Hijji, B. Barare, A.P. Kennedy, R. Butcher, Sensor Actuat. B-Chem. 136 (2009) 297–302;
(c) Y. Li, J. Li, H. Lin, J. Shao, Z.-S. Cai, H. Lin, J. Lumin. 130 (2010) 466–472.
[12] (a) V. Reena, S. Suganya, S. Velmathi, J. Fluorine Chem, 2013 (in press).;
(b) D. Sharma, R.K. Bera, S.K. Sahoo, Spectrochim. Acta A 105 (2013) 477–482;
(c) S.L. Ashok Kumar, M.S. Kumar, P.B. Sreeja, A. Sreekanth, Spectrochim. Acta A 113 (2013) 123–129;
(d) J. Li, H. Lin, Z. Cai, H. Lin, Spectrochim. Acta A 72 (2009) 1062–1065;
(e) J. Shao, Y. Qiao, H. Lin, H. Lin, Spectrochim. Acta A 71 (2009) 1736–1740;
(f) J-Q. Li, T-B. Wei, Q. Lin, P. Li, Y-M. Zhang, Spectrochim. Acta A 83 (2011) 187–193.
[13] A.A. Gabr, Spectrochim. Acta A 46 (1990) 1751–1757.
[14] Q. Li, Y. Guo, J. Xu, S. Shao, J. Photochem. Photobiol., B 103 (2011) 140–144.
[15] M.-X. Liu, T.-B. Wei, Q. Lin, Y.-M. Zhang, Spectrochim. Acta A 79 (2011) 1837–1842.
[16] (a) J. Shao, M. Yu, H. Lin, H. Lin, Spectrochim. Acta A 46 (1990) 1751–1757;
(b) S. Hu, Y. Guo, J. Xua, S. Shao, Org. Biomol. Chem. 6 (2008) 2071–2075.